*Anal. Chem.* **2002,** *74,* 5099−5104

# Coupled Electrorotation of Polymer Microspheres for Microfluidic Sensing and Mixing

Clyde F. Wilson,[†] Mark I. Wallace,[†] Keisuke Morishima,[‡] Garth J. Simpson,[§] and Richard N. Zare*,[†]

*Department of Chemistry, Stanford University, Stanford, California 94305-5080, Kanagawa Academy of Science and Technology (KAST), KSP West 614, 3-2-1 Sakado, Takatsu-ku, Kawasaki-shi, Kanagawa 213-0012, Japan, and Department of Chemistry, Purdue University, West Lafayette Indiana 47907-1393*

**We show that coupled electrorotation (CER) of microscopic particles using microfabricated electrodes can be used for localized sensing and mixing. The effective use of microelectromechanical systems and micro total analysis systems requires many types of control. These include the ability to (1) manipulate objects within microchannels by noncontact means, (2) mix fluids, and (3) sense local chemical parameters. Coupled electrorotation, in which the interactions between induced electric dipoles of adjacent particles lead to particle rotation, addresses aspects of all three challenges simultaneously. CER is a simple means of controlling the rotation of dielectric objects using homogeneous external radio frequency electric fields. CER is sensitive to several chemical and physical parameters such as the solution conductivity, pH, and viscosity. As a step toward integrating CER devices into microfluidic systems, a simple chip was designed to induce local mixing and to detect local changes in salt concentration, pH, and viscosity.**

Electric fields have proven instrumental for the manipulation of microscale objects. Electrokinetic forces on a dielectric object in an electric field can be classified as producing either translational or rotational motion.[1] Translational motions can be induced by spatially homogeneous or inhomogeneous electric fields and are respectively termed electrophoresis and dielectrophoresis. Rotational motion is dependent on the formation of a dipole in the object to be rotated and the application of a torque to that dipole by an electric field. In electrorotation, a rotating electric field both induces dipole moments in particles and exerts a torque on the induced dipole moments, causing the particles to rotate. In coupled electrorotation (CER), the externally applied field is static and fixed in space. Dipoles are induced in two or more adjacent particles. A time delay exists in the buildup and decay of the dipole moments. Consequently, the electric field has in general two oscillating components offset in phase, one along the static field direction and one perpendicular to it. The sum of the two oscillating electric fields generates a rotating electric field that acts on each particle. The interaction between the two dipoles is akin to the interaction between two bar magnets. In the case that one of the objects cannot rotate, dipoles are still induced and torques are still applied but only to the object that is free to rotate. The latter occurs when a microsphere is adjacent to a glass or polymer microstructure, for example.

Electrophoresis and dielectrophoresis have been the subject of extensive study for the manipulation of particles in microelectromechanical systems (MEMS) devices. For example, electrophoresis has been used for electroosmotic pumping[2] and chemical separations[3] in MEMS devices. Dielectrophoresis has been used to trap and manipulate cells,[4,5] viruses,[6] and DNA.[7] Traveling wave dielectrophoresis has also been used to separate and move particles in a microfluidic device.[8]

In contrast, the application of electrorotation to microfluidic analysis is relatively new. Historically, electrorotation has been used to characterize the properties of cells.[9,10] Electrorotation has also been used to assess the viability of cells in real time, as it provides a measure of membrane integrity.[11] More recently, this application has been implemented in a MEMS device to characterize the cytoplasmic properties of cells.[12] Schnelle et al. have combined electrorotation in a quadrupole field with optical tweezers,[13] allowing the simultaneous trapping and manipulation (translational and rotational) of particles.

The first demonstration of CER (two or more objects coupling to each other) was made by Teixeira-Pinto et al.[14] in which *Euglena* and pseudopod fragments were observed to rotate spontaneously

* To whom correspondence should be addressed. E-mail: zare@stanford.edu.
[†] Stanford University.
[‡] Kanagawa Academy of Science and Technology.
[§] Purdue University.

(1) Goater, A. D.; Pethig, R. *Parasitology* **1998**, *117*, S177−S189.
(2) SalimiMoosavi, H.; Tang, T.; Harrison, D. J. *J. Am. Chem. Soc.* **1997**, *119*, 8716−8717.
(3) Manz, A.; Effenhauser, C. S.; Burggraf, N.; Harrison, D. J.; Seiler, K.; Fluri, K. *J. Micromech. Microeng.* **1994**, *4*, 257−265.
(4) Jones, T. B. *Electromechanics of Particles*; Cambridge University Press: New York, 1996.
(5) Mahaworasilpa, T. L.; Coster, H. G. L.; George, E. P. *Biochim. Biophys. Acta: Biomembr.* **1994**, *1193*, 118−126.
(6) Morgan, H.; Green, N. G. *J. Electrostat.* **1997**, *42*, 279−293.
(7) Asbury, C. L.; van den Engh, G. *Biophys. J.* **1998**, *74*, 1024−1030.
(8) Cui, L.; Holmes, D.; Morgan, H. *Electrophoresis* **2001**, *22*, 3893−3901.
(9) Arnold, W. M.; Zimmermann, U. *Z. Naturforsch. C: J. Biosci.* **1982**, *37*, 908−915.
(10) Mischel, M.; Voss, A.; Pohl, H. A. *J. Biol. Phys.* **1992**, *10*, 223−226.
(11) Goater, A. D.; Burt, J. P. H.; Pethig, R. *J. Phys. D: Appl. Phys.* **1997**, *33*, L65-L70.
(12) Reichle, C.; Schnelle, T.; Müller, T.; Leya, T.; Fuhr, G. *Biochim. Biophys. Acta* **2000**, *1459*, 218−229.
(13) Schnelle, T.; Müller, T.; Reichle, C.; Fuhr, G. *Appl. Phys. B: Lasers Opt.* **2000**, *70*, 267−274.
(14) Teixeira-Pinto, A. A.; Kejelski, L. L., Jr.; Culter, J. L.; Heller, J. H. *Exp. Cell Res.* **1960**, 20, 548.

10.1021/ac0258599 CCC: $22.00 
Published on Web 08/29/2002

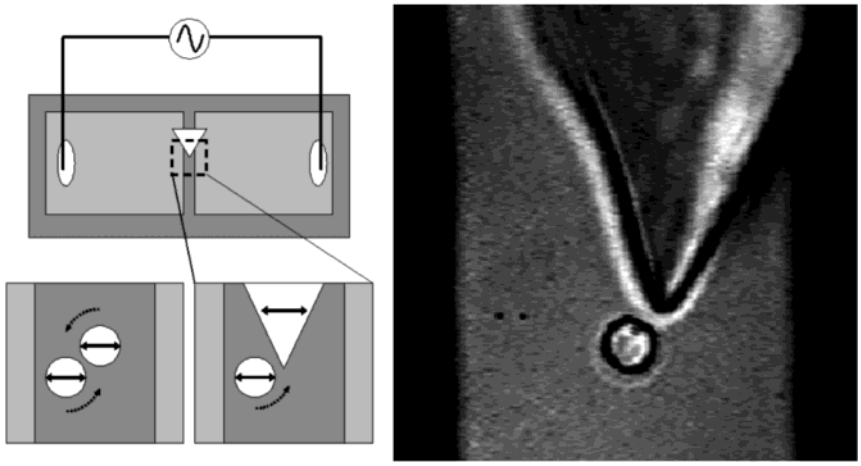

Figure 1. Microfabricated chips used to apply an electric field to two adjacent microspheres (for sensing experiments, not shown in this figure) or a microsphere adjacent to a PDMS corner (for mixing experiments). Wires connecting the function generator to the electrodes were attached to the latter using conductive epoxy (ovals). For a description of chip manufacture see text.

in strong rf fields when adjacent to a larger amoeba. Holzapfel et al.[15] and Mahaworasilpa et al.[16] presented theoretical formalisms to treat CER in an ac field. In recent work, we have combined CER with optical trapping and photopatterning to quantify rotation of submicrometer particles, fabricate microscopic "antigears," and demonstrate the possibility of exploiting the registry of sphere rotation rates in performing local sensing.[17] However, the instrumentation we used for inducing CER in this earlier work, in which microelectrodes were positioned using micromanipulators, was not ideally suited for direct incorporation into microfluidic devices. In addition, we demonstrated that a sealed pipet tip can induce a torque on a microsphere undergoing CER with another microsphere, but we had not used a stationary object to induce CER in a single microsphere.

Additional mechanisms to affect rotation of microscopic particles include all optical methods such as radiation pressure on microfabricated rotors,[18] the trapping of birefringent particles,[19] the use of Laguerre−Gaussian laser modes,[20] the use of optically trapped magnetic particles in rotating electromagnetic fields,[21] and the fabrication of electrostatic or magnetic micromotors.[22] Advantages of CER over these methods include the simplicity of the system needed to establish CER and the number of tasks that can be accomplished by CER simultaneously.

In this work, CER on a chip is demonstrated using microfabricated electrodes and optical tweezers to induce controlled rotation in individual pairs of microscopic objects. The coupled electrorotation rates of polystyrene microspheres were measured as a function of viscosity, NaCl concentration, and pH. The results compared closely with theoretical models. The chip structures used to perform these measurements are well-suited for incorporation into more complex microfabricated devices. CER is achieved between a microsphere and an adjacent immobilized polymer microstructure. Application of CER for microfluidic mixing and sensing was also investigated.

## EXPERIMENTAL SECTION

Particle rotation measurements were made using an apparatus similar to that described previously.[17] Briefly, images were acquired using a Nikon Diaphot inverted microscope, collected by a silicon-intensified target (SIT, Hamamatsu C2400-08) camera, and recorded onto videotape. Dual optical trapping was achieved using a 985-nm MOPA diode laser (1 W, SDL model 5762-A6) split into its two polarization components. Each trap could be manipulated independently. A dichroic mirror allowed the introduction of both the optical trapping beams and the 488-nm excitation beam from an argon ion laser (SpectraPhysics Stabilite 2017. Microchips (see Figure 1) were constructed by sputtering gold (Hummer V Gold Sputter Coater, Technics, Inc., CA) onto glass coverslips (24 × 60 mm, No. 1, VWR Scientific, Inc., West Chester, PA) to a final thickness of ∼100 nm. Photolithography was then used to etch a 10-$\mu$m gap to separate the sputtered region into two equal halves, creating two electrodes of roughly equal size. Prior to sputtering, the glass coverslips were cleaned with methanol, 2-propanol, and acetone.

The chip was mounted over the oil immersion objective and a droplet (14−50 $\mu$L) of 2-$\mu$m latex spheres suspended in water was placed on the chip such that the drop was in contact with both gold electrodes. The latex spheres were Yellow-green carboxylate FluoSpheres (Molecular Probes, Eugene, OR) for sensing experiments and Polybead Carboxylate Microspheres (Polysciences, Inc., Warrington, PA) for mixing experiements. The latex spheres were diluted by a factor of ∼100. The latex spheres from Molecular Probes are suspended in 2 mM sodium azide. We did not perform additional purification; the latex sphere solution used in the sensing experiments contained ∼20 nM sodium azide. To achieve consistent results, the relative position of the microspheres in the optical traps was not changed during individual experiments.


(15) Holzapfel, C.; Vienken, J.; Zimmermann, U. *J. Membr. Biol.* **1982**, *67*, 13.
(16) Mahaworasilpa, T. L.; Coster, H. G. L.; George, E. P. *Biochim. Biophys. Acta: Biomembr.* **1996**, *1281*, 5−14.
(17) Simpson, G. J.; Wilson, C. F.; Gericke, K.; Zare, R. N. *ChemPhysChem* **2002**, *3*, 416−423.
(18) Ukita, H.; Kanehira, M. *IEEE J. Sel. Top. Quantum Electron.* **2002**, *8*, 111−117.
(19) Friese, M. E. J.; Nieminen, T. A.; Heckenberg, N. R.; Rubinsztein-Dunlop, H. *Nature* **1998**, *394*, 348−350.
(20) Paterson, L.; MacDonald, M. P.; Arlt, J.; Sibbett, W.; Bryant, P. E.; Dholakia, K. *Science* **2001**, *292*, 912−914.
(21) Sacconi, L.; Romano, G.; Ballerini, R.; Capitanio, M.; De Pas, M.; Giuntini, M.; Dunlap, D.; Finzi, L.; Pavone, F. S. *Opt. Lett.* **2001**, *26*, 1359−1361.
(22) Judy, J. W. *Smart Mater. Struct.* **2001**, *10*, 1115−1134.

Changes in the distance between microspheres results in significant changes in rotation rate.

The effects of solution conductivity, pH, and viscosity on CER were then measured. Experimental procedure was as follows: (1) two microspheres were immobilized in the dual optical trap with one microsphere (M1) positioned at the focal point of the excitation laser, (2) M1 was partially photoaltered with focused 488-nm light for 0.1 s, (3) a 500-kHz, 60 kV $cm^{-1}$ electric field sine wave was applied across the microsphere pair (see below) after 3 min had passed from the time of placing the drop on the chip to ensure uniform and minimal evaporation between trials, and (4) LIF measurements were acquired for 1 min with wide-field 488-nm excitation by passing the excitation beam through a spinning disk diffuser. Microsphere photoalteration (bleaching) allowed visualization of rotation.[23] The bleaching time for beads was selected to be less than the time required for the microsphere to undergo rotational diffusion by more than a few degrees. The chip was rinsed three times with drops the same size as those used in the experiments. Rinsing was done with the same solution used in the following trial. Mixing experiments were performed by replacing one microsphere with a poly(dimethylsiloxane) (PDMS) wedge mounted between the electrodes. Drop sizes used for the experiments were ~50 $\mu$L for mixing experiments, 30 $\mu$L for pH measurements, and 14 $\mu$L for salt and viscosity measurements. Experiments taking longer than a few minutes to perform or those involving pH measurements were in general done with larger drop volumes to minimize effects from drop evaporation.

The rf output from a Stanford Research Systems function generator was coupled directly to the microelectrodes. Wires were attached to the electrodes with conductive epoxy (Circuitworks CW2400, Chemtronics, Kennesaw, GA). The use of 500 kHz optimized sphere rotation and provided a slight dielectrophoretic repulsion to minimize interference from stray microspheres floating into the trapping region. Consistent with previous findings,[24−26] isolated, single spheres did not rotate under these conditions, confirming that electroosmotic flow is unimportant in these experiments.

Rotation rates did not change significantly over the time scales used for data acquisition (i.e., a few minutes or less). Evaporation of the droplet resulted in noticeable changes in the rotation rates for longer times (between 15 min to well over 3 h, depending on the droplet size).

Visualization of local mixing was achieved by adding 500-nm tracer particles (Yellow-green carboxylate FluoSpheres, Molecular Probes) to an aqueous solution of 2-$\mu$m spheres (described above). In this solution, a 2-$\mu$m polystyrene microsphere is subject to a 500-kHz, 60 kV $cm^{-1}$ electric field sine wave while in close proximity to a static PDMS structure. The PDMS structure was a sharp corner made by simply cutting a piece of PDMS with a razor blade and placing the corner on the gap between the electrodes. The presence of this PDMS corner induced CER in microspheres. Local fluid flow was visualized by direct observation of the trajectories of individual tracer particles.

## THEORY

DEP and CER forces are principally determined by conductivity in the surface layer of a particle.[27−29] This surface layer describes a thin three-dimensional shell containing the charged groups in the solvent double layer, at the particle surface, and within a thin layer below the particle surface that is accessible to solvent.[30] Upon application of a locally homogeneous rf electric field, a dipole is created within the particle.

Dielectrophoresis and electrorotation are related by the respective real and imaginary components of the Claussius−Mossotti factor in the equations describing the forces upon a particle. For the case of an ideal sphere, the dielectric force is[31]

$$F = 2\pi r^3 \epsilon_m \epsilon_0 \mathrm{Re}[f(\omega)] \nabla E^2 \quad (1)$$

For electrorotation, the torque is[31]

$$\Gamma = -4\pi r^3 \epsilon_m \epsilon_0 \mathrm{Im}[f(\omega)] E^2 \quad (2)$$

where $\epsilon_m$ is the relative dielectric constant of the suspension medium, $\epsilon_0$ is the permittivity of free space, $r$ is the particle radius, $E$ is the amplitude of the driving field, and $f(\omega)$ is the Claussius−Mossotti factor, dependent on $\omega$, the angular frequency of the field.[31]

$$f(\omega) = (\epsilon_p^* - \epsilon_m^*)/(\epsilon_p^* + 2\epsilon_m^*) \quad (3)$$

Here $\epsilon_p^*$ and $\epsilon_m^*$ are the effective relative complex permittivities of the particle and the medium. An effective permittivity can be used to model the properties of a particle as a homogeneous sphere with equivalent dielectric properties. A more accurate description of microsphere properties should use a surface-layer model of microsphere conductivity and permittivity.[30]

The relative complex permittivity is described by

$$\epsilon^* = \epsilon - i\sigma/\omega\epsilon_0 \quad (4)$$

where $\epsilon$ is the real relative permittivity and $\sigma$ is the medium conductivity.

Assuming a Stokes−Einstein model of the solution viscosity, the angular velocity $\Omega$ for one particle in a pair of identical particles subject to CER can be described by[16]

$$\Omega = \frac{3\epsilon_m}{8\eta} E^2 \sin 2\theta \left[\frac{\mathrm{Im}[f(\omega)]}{4 - \mathrm{Re}[f(\omega)]}\right]. \quad (5)$$

Here, $\eta$ is the viscosity of the solution medium, $E$ is the applied alternating external electric field, and $\theta$ is the angle between the applied field and the vector connecting the centers of the two particles.


(23) Simpson, G. J.; Wohland, T.; Zare, R. N. *Nano Lett.* **2002**, *2*, 207−210.
(24) Grosse, C.; Shilov, V. N. *Colloids Surf. A* **1998**, *140*, 199.
(25) Grosse, C.; Shilov, V. N. *J. Phys. Chem.* **1996**, *100*, 1771−1778.
(26) Neu, B.; Georgieva, R.; Bäumler, H.; Shilov, V. N.; Knippel, E.; Donath, E. *Colloids Surf. A* **1998**, *140*, 325.
(27) Fuhr, G.; Kuzmin, P. I. **1986**, *Biophys. J* . 50, 789−795.
(28) Sauer, F. A.; Schlogl, R. W. In *Interactions between Electromagnetic Fields and Cells*; Chiabrere, A., Nicolini, C., Schwan, H. P., Eds.; Plenum Press: New York, 1985; pp 203−251.
(29) Arnold, W. M.; Schwan, H. P.; Zimmermann, U. *J. Phys. Chem.* **1987**, *91*, 5093−5098.
(30) Maier, H. *Biophys. J.* **1997**, *73*, 1617−1626.
(31) Arnold, W. M.; Zimmermann, U. *J. Electrostat.* **1988**, *21*, 151−191.

For the case of two different spheres, the ratio of angular velocities becomes[17]

$$\frac{\Omega_A}{\Omega_B} \cong \frac{\mathrm{Im}[f_A(\omega)]}{\mathrm{Im}[f_B(\omega)]}\left(\frac{\mathrm{Im}[f_B(\omega)] + (R_A/r)^3\mathrm{Im}[f_A(\omega)f_B(\omega)]}{\mathrm{Im}[f_A(\omega)] + (R_B/r)^3\,\mathrm{Im}[f_A(\omega)f_B(\omega)]}\right) \quad (6)$$

where $R$ is the radius of the sphere, $r$ is the distance between the spheres, and A and B are subscripts that denote the two different spheres.

Describing the two particles in terms of equivalent homogeneous spheres, and in the case of identical particles with frequency independent permittivities and conductivities, the real and imaginary parts of the Claussius−Mossotti factor become

$$\mathrm{Re}[f(\omega)] = \frac{\sigma_p^2 + \sigma_p\sigma_m - 2\sigma_m^2 + \omega^2(\epsilon_p - \epsilon_m)(\epsilon_p - 2\epsilon_p)}{(\sigma_p + 2\sigma_m)^2 + \omega^2(\epsilon_p + 2\epsilon_m)^2} \quad (7)$$

$$\mathrm{Im}[f(\omega)] = \frac{3\omega(\epsilon_m\sigma_p - \epsilon_p\sigma_m)}{(\sigma_p + 2\sigma_m)^2 + \omega^2(\epsilon_p + 2\epsilon_m)^2} \quad (8)$$

These equations follow from the theory of Lampa,[32] describing the torque exerted by a rotating field on a sphere as described in the review of Arnold and Zimmerman.[31] We substitute eqs 7 and 8 into eq 5 to predict the variation in rotation rate with viscosity and salt concentration.

## RESULTS AND DISCUSSION

The variation of microsphere angular velocity with solution viscosity is shown in Figure 2. The expected $1/\eta$ dependence of rotation rate is observed. The solid line in Figure 2 corresponds to a nonlinear least-squares fit of the data to a model describing CER in terms of two equivalent homogeneous spheres. Both the variation in solution conductivity and dielectric permittivity are taken into account.[33] Changes in permittivity are assumed to follow the Rayleigh model for the mixing of a two-component, one-phase system of dielectric materials;

$$\frac{\epsilon_{12} - 1}{\epsilon_{12} + 2} = \phi_1\frac{\epsilon_1 - 1}{\epsilon_1 + 2} + \phi_2\frac{\epsilon_2 - 1}{\epsilon_2 + 2} \quad (9)$$

where $\epsilon_m$ is the dielectric constant of the mixture; $\epsilon_1$, $\epsilon_2$, $\phi_1$, and $\phi_2$ are respectively the dielectric constant and volume fraction of the two components. Under the conditions used for these experiments, a change in viscosity of $5 \times 10^{-4}$ kg m$^{-1}$ s$^{-1}$ is detected as ethylene glycol is added to the aqueous solution until roughly one-quarter of the solution is ethylene glycol. The rotation rate continues to fall, but the ability to detect changes in viscosity falls off dramatically. Thus, the dynamic range for these measurements when used as a viscometer is within ~40% of the viscosity of water. Changing the experimental conditions, such as increasing the electric field strength, would increase the absolute CER rotation rate, thereby increasing the dynamic range over which viscosity can be measured.

(32) Lampa, A. *Wien. Ber. 2a* **1906**, *115*, 1659−1690.
(33) Tsierkezos, N. G.; Molinou, I. E. *J. Chem. Eng. Data* **1998**, *43*, 989−993.

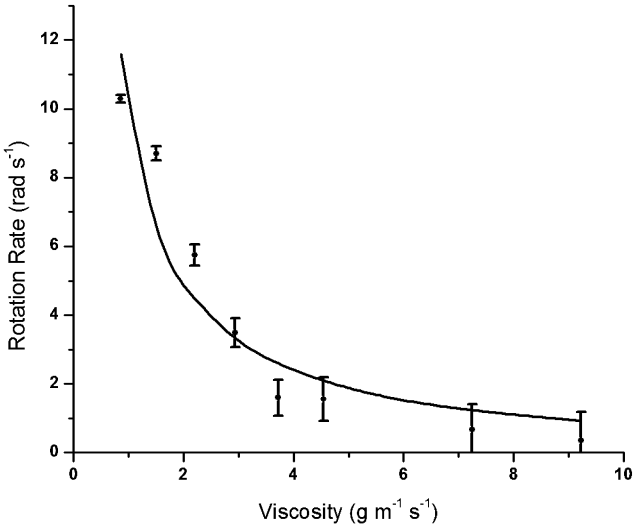


Figure 2. Variation of microsphere angular velocity with solution viscosity. The solid line corresponds to a nonlinear least-squares fit of the data to a model describing CER in terms of two equivalent homogeneous spheres. Variations in both solution conductivity and dielectric permittivity are taken into account. Fitting parameters: $E$ = V m$^{-1}$, $\theta = \pi/4$, $\omega = 3.14 \times 10^6$ rad s$^{-1}$, and $\sigma_m = 2.5 \times 10^{-4}$ S m$^{-1}$. A Rayleigh model of dielectric mixtures is used to describe the changes in solution permittivity. The fitted effective microsphere conductivity and relative permittivity are $\sigma_p = 6.2 \times 10^{-4}$S m$^{-1}$ and $\epsilon_p = 18.8$, respectively.

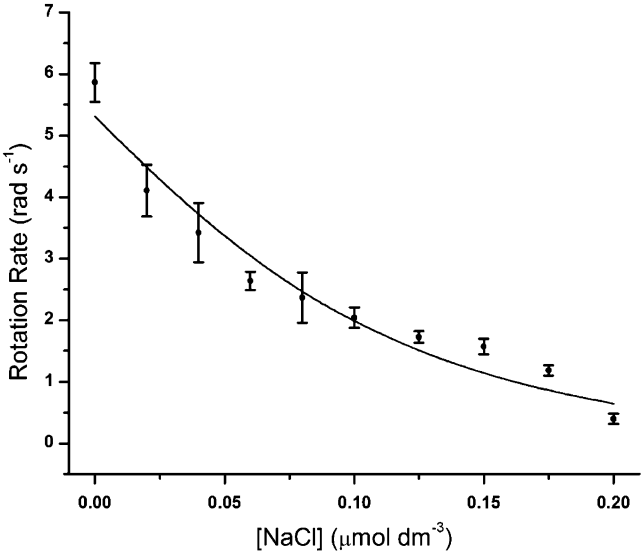


Figure 3. Variation of microsphere angular velocity with solution NaCl concentration. The solid line corresponds to a nonlinear least-squares fit of the data to a model describing CER in terms of two equivalent homogeneous spheres. Fitting parameters: E = $10^5$ V m$^{-1}$, $\theta = \pi/4$, $\omega = 3.14 \times 10^6$ rad s$^{-1}$, and $\eta = 8.57 \times 10^{-4}$ kg m$^{-1}$ s$^{-1}$. The fitted effective microsphere conductivity and relative permittivity are $\sigma_p = 3.5 \times 10^{-4}$ S m$^{-1}$ and $\epsilon_p = 2.2$, respectively.

Figure 3 shows the dependence of rotation rate on the concentration of NaCl. Again, the solid line corresponds to a nonlinear least-squares fit using a model describing CER in terms of two equivalent spheres. Solution viscosity and dielectric permittivity are assumed constant. Under the conditions used for these experiments, changes in NaCl concentration of 40 nM were detected with a dynamic range of 0−200 nM in added salt corresponding to a conductivity range between 6 and 29 $\mu$S cm$^{-1}$.

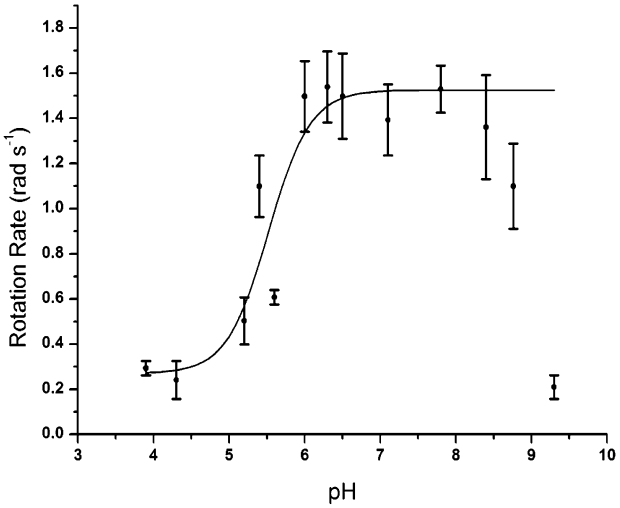


Figure 4. Variation of microsphere angular velocity with solution pH. The solid line corresponds to a nonlinear least-squares fit of the data to a sigmoid below pH 8. The p$K_a$ of this fit is 5.5. The decrease in rotation rate at pH greater than 8 is caused by the change in conductivity as the ionic strength of the solution increases.

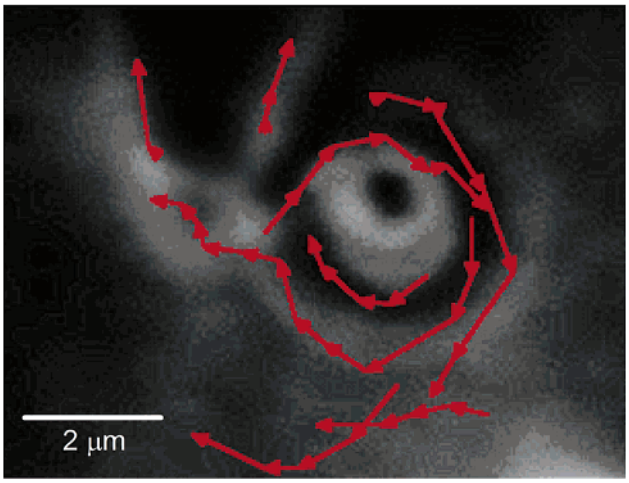


Figure 5. Visualization of local mixing around a polystyrene sphere in close proximity to a PDMS microstructure. Nine sample trajectories of fluorescent tracer particles are shown, demonstrating the local fluid flow around the rotating microsphere. Each vector represents a time interval of 33.3 ms. Bar is 2 $\mu$m.

Measurable electrorotation and CER of polymer beads is not expected to occur under physiological conditions using reasonable field strengths. Nevertheless, electrorotation[9−12] and CER[14,15] of cells have been accomplished using sugar (or sugar alcohol) solutions of low ionic strength.

Figure 4 depicts the variation in rotation rate with solution pH. The value of the pH was varied by addition of 0.25 M NaOH to a 5-mL unbuffered solution of microspheres whose initial pH was set at 3.9 by the addition of ∼0.1 $\mu$L of 37% HCl to a 225-mL stock solution. The conductivities for solutions similar to those used in the CER pH experiments were 55 $\mu$S cm$^{-1}$ for pH 3.7, 29 $\mu$S cm$^{-1}$ for pH 4.4, and 32 $\mu$S cm$^{-1}$ at pH 9.8. The conductivity was 24 $\mu$S cm$^{-1}$ for pH 5.2, 6.5, 7.3, and 8.6. The solid line in Figure 3 describes a sigmoid fit to the pH changes below pH 8. This fit describes a simple mass balance between dissociation of protons from surface-bound carboxyl groups into the solution. The p$K_a$ of this reaction is initially 5.5 ± 0.2. This model does not take into account any dispersion in surface charge concentration. As the carboxy groups on the surface of the microsphere deprotonate, the increasing surface charge resists further deprotonation. The final carboxy groups to deprotonate have a p$K_a$ of ∼10. The decrease in rotation rate at high pH is caused by the change in solution conductivity as the ionic strength of the solution increases. The high solution conductivities present when buffers are used to control pH reduce the rotation rate (similar to what is observed in Figure 3). Hence, buffers could not be used to stabilize the pH for these experiments and this may have contributed to the error in these measurements.

The ability to sense local variations in pH, conductivity, or salt concentration might be useful in work that requires specific conditions to function effectively. Maintaining optimum solubility of specific chemical species, optimizing chemical separation conditions, or ensuring that proper reaction conditions exist within a microfluidic system would be facilitated by improved local sensing capabilities. In addition, local sensing could provide improved information on how specific materials or surfaces within microfluidic devices alter the solution chemistry within the channels they contain (such as by leaching, adsorption, or absorption). Local sensing could also be an indicator for the effectiveness of cleaning or flushing processes. The simplicity of a CER microfluidic sensor also suggests that it might be used in a parallel manner to detect gradients in solution properties. Such a modification would only require the use of multiple optical traps.

The results depicted in Figure 5 demonstrate that CER can be used to affect mass transport and mixing at microscopic length scales, suggesting direct applications for mixing devices in chips. Fluid flow within a microfluidic device is in the low Reynolds number regime.[34,35] As viscous rather than inertial effects control the fluid motion in this regime, mixing is dominated by diffusion. The ability to overcome the limitations of diffusional mixing and produce local turbulence is a key hurdle in the successful implementation of microfluidic devices. Alternative methods currently used to produce local microfluidic mixing include the use of charged surfaces,[36] t-junctions,[37] pulsatile flow,[38] acousto-fluidics,[39] optically driven microfabricated rotors,[40] or relief structures on the inner walls of the microchannel (e.g., ridges[41] or helical structures[42]). CER may have several distinct advantages over many of these methods. For example, CER can be used to mix a localized region of fluid with dimensions smaller than 1 $\mu$m. Physical contact is not needed between the mixing device and the chip as it is with microfabricated rotors. No special

(34) Purcell, E. M. *Am. J. Phys.* **1977**, *45*, 3−11.
(35) Brody, J. P.; Yager, P.; Goldstein, R. E.; Austin, R. H. *Biophys. J.* **1996**, *71*, 3430−3441.
(36) Kuksenok, O.; Yeomans, J. M.; Balazs, A. C. *Langmuir* **2001**, *17*, 7186−7190.
(37) Johnson, T. J.; Ross, D.; Locascio, L. E. *Anal. Chem.* **2002**, *74*, 45−51.
(38) Lee, B. S.; Kang, I. S.; Lim, H. C. *Int. J. Heat Mass Transfer* **1999**, *42*, 2571−2581.
(39) Rife, J. C.; Bell, M. I.; Horwitz, J. S.; Kabler, M. N.; Auyeung, R. C. Y.; Kim, W. J. *Sens. Actuators, A* **2000**, *86*, 135−140.
(40) Ukita, H.; Kanehira, M. *IEEE J. Sel. Top. Quantum Electron.* **2002**, *8*, 111−117.
(41) Stroock, A. D.; Dertinger, S. K. W.; Ajdari, A.; Mezic, I.; Stone, H. A.; Whitesides, G. M. *Science* **2002**, *295*, 647−651.
(42) Liu, R. H.; Stremler, M. A.; Sharp, K. V.; Olsen, M. G.; Santiago, J. G.; Adrian, R. J.; Aref, H.; Beebe, D. J. J. *Microelectromech. Syst.* **2000**, *9*, 190−197.

processing is needed to create a microscopic mixer, and polymer beads are readily available and easily used. Mixing can also be turned on and off as required, as opposed to the mixing achieved by a static structure. The positioning of the microsphere(s) is readily adjustable, depending on the geometry of the applied electric field and the range of movement of the optical trap holding the microsphere(s). This flexibility allows some level of control of the region to be mixed. A more quantitative investigation of CER-induced local mixing could be achieved using particle image velocimetry.

In summary, we have developed a microchip to optimize the use of CER for sensing local changes in salt concentration, viscosity, and pH (the three parameters that have the greatest impact on the efficiency of CER). Changes in the rates of microsphere CER were used to detect 40 nM changes in salt concentration, $5 \times 10^{-4}$ kg $m^{-1}$ $s^{-1}$ changes in viscosity, and 0.2 pH unit changes in the region of the p$K_a$ of the microsphere. The microchip was also used to demonstrate microfluidic mixing induced by CER between a microsphere and a PDMS microstructure. Taken together, CER is a versatile and simple tool that simultaneously allows for the sensitive control of particle rotation and microfluidic mixing and has applications in chemical sensing within microfluidic systems. Its major drawback, at present, is the need to operate CER at low ionic strength.

## ACKNOWLEDGMENT

We thank Thorsten Wohland and Rebecca Whelan for their assistance. C.F.W. expresses his thanks for a DuPont Pharmaceutical Graduate Fellowship and G.J.S. for a Pfizer and the Life Sciences Research Foundation Postdoctoral Fellowship. This work was supported by the National Science Foundation under NSF 00-119.

Received for review June 12, 2002. Accepted July 31, 2002.

AC0258599